Geophysical Prospecting, 1998, **46**, 105–120

Very high resolution 3D marine seismic data processing for geotechnical applications[1]

B. Marsset,[2] T. Missiaen,[2] Y.-H. De Roeck,[2] M. Noble,[3] W. Versteeg[4] and J.P. Henriet[4]

Abstract

The processing of a small-scale, very high resolution (VHR) shallow marine 3D data volume is described. The data were acquired over a small clay diapir, on the river Schelde, in 1990. Using an array of 12 dual-channel microstreamers towed from a catamaran, a network of 1 m × 1 m bins could be produced over an area of 50 m × 180 m (< 100 m penetration). Positioning was performed with an auto-tracking laser ranging system, assuring an absolute accuracy of a few decimetres.

Preliminary processing steps included tidal correction and multiple removal. An important step concerned the application of 3D prestack Kirchhoff depth migration. Indeed this processing allows easy handling of the exact positions of both source and receivers as the latter were not set out on a conventional regular grid due to navigation difficulties. Because of the restricted data volume and the more-or-less stratified medium, a 1D velocity model could be used. This allowed a considerable simplification of the migration algorithm, based on summation. Traveltimes were calculated only once, using a 2D time grid with 0.1 m intervals.

This migration method proved very efficient, greatly improving the seismic image, and involved only limited CPU time on a small computer (Sparc 10 workstation). It clearly demonstrates that advanced seismic processing can form a valuable and economically feasible tool for VHR shallow subsurface 3D seismics, as long as the velocity field is not too complex. This method should therefore no longer be restricted to large computers and hydrocarbon exploration, but should also become a routine for VHR 3D shallow seismic work.

Introduction

Very high resolution (VHR) marine seismic data are widely used both in the field of engineering geophysics as well as in geological and environmental site investigations. This technology has progressed quickly. Evolution towards cheaper and more

[1] Received March 1996, revision accepted August 1997.
[2] IFREMER, Centre de Brest, BP 70, 29280 Plouzane, France.
[3] Ecole des Mines de Paris, 77305 Fontainebleau, France.
[4] RCMG, Universiteit Gent, 9000 Gent, Belgium.

powerful computers is making VHR multichannel recording more popular. Whereas 2D surveys are now in common use, most 3D acquisition is still carried out only in the hydrocarbon exploration realm. It involves complex field and processing procedures, making it very costly and time-consuming.

In recent years, the Renard Centre of Marine Geology (University of Gent, Belgium) has scaled down the shallow marine 3D method to very high resolution, thereby entering the world of small-scale geological structures. Using a relatively simple acquisition system, a small 3D data volume (lateral dimensions 50 m × 180 m, penetration < 100 m) was acquired over a clay diapir under the river Schelde. Time slices obtained after stacking showed a resolution never achieved previously in 3D practice (Henriet, Verschuren and Versteeg 1992).

Up to now, the processing sequence of shallow seismic data has often seemed to stagnate around the 1D assumption of the common depth point. Indeed very few people in this field go beyond NMO and stack. The sea-bed and its near-subsurface, however, are, by nature, 2- and often 3-dimensional structures and should be treated as such. This can be done by applying migration algorithms to the data. This imaging technique, coming directly from the oil industry, has the well-established reputation of being difficult to use and requiring large computer resources. Nowadays this is no longer true, due not only to faster processors but also to new algorithms.

The aim of this paper is not to give a full detailed discussion of the 3D migration technique. Several authors have written excellent articles and books covering this topic, and in many cases have done so with considerable rigour. Our motivation for writing this paper came from the belief that practical advice for the application of 3D prestack migration for near-subsurface seismic data is in short supply. We prove here that migration forms an essential processing step involving only moderate supplementary costs, and it should therefore become a routine procedure for VHR 3D shallow seismic work.

Target

The target consisted of a small diapir under the river Schelde near Antwerp, close to the site proposed for a metro tunnel. The clay beds are marked by a large number of concretions, with diameters ranging between 0.5 m and 1 m and thicknesses between 0.2 m and 0.3 m. Both the structural deformation and the presence of concretion beds motivated a detailed seismic and geotechnical survey of the tunnel site (Schittekat, Henriet and Vandenberghe 1983). These detailed site investigations made the area a well-documented test ground to evaluate the capabilities of VHR 3D seismic reflection imaging in geotechnical applications. This survey was carried out in 1990, in the framework of an EEC-supported programme for the stability evaluation of potential offshore sites.

The diapir in the Rupelian (Oligocene—middle Tertiary) clay has an apparent diameter of 60 m, and a vertical amplitude increasing from a few decimetres at 50 m depth to a few metres at about 25 m depth. As the lowest horizons do not appear to be

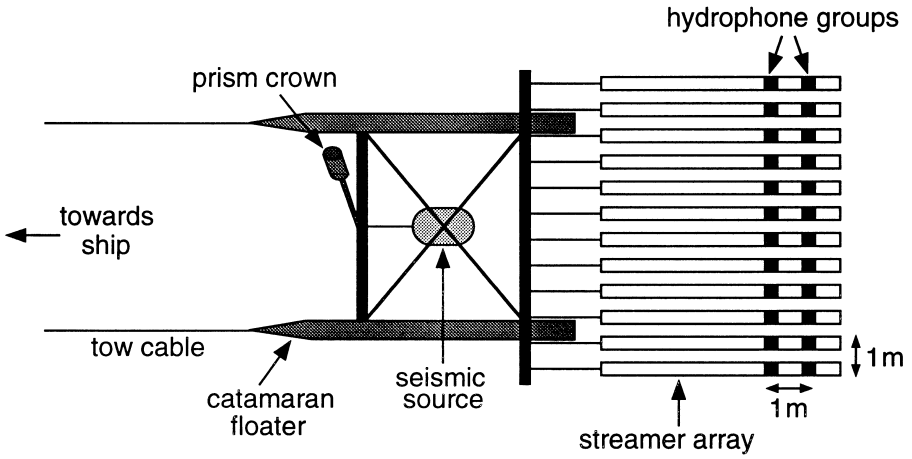

Figure 1. Schematic overview of the 3D seismic acquisition system 'SEISCAT".

significantly deformed below the diapir, the effect of velocity pull-up can probably be ruled out. The origin of the diapir is thought most likely to be related to decompaction, the sediment load being reduced by erosion of the river bed (Verschuren 1992). The concretions in the clay beds, which have a diameter of 0.5–1 m and a thickness of 0.2–0.3 m, locally stand out as diffraction clusters on analogue boomer profiles recorded during former seismic surveys (Hemerijckx *et al.* 1983).

Data acquisition

In order to allow accurate imaging of the diapiric deformation and the larger clay concretions, the 3D acquisition on the river Schelde was planned with a bin size of 1 metre (Henriet *et al.* 1992). Since the depth of the target is extremely shallow (about 25 m), this would give moderate oversampling of the first Fresnel zone of 4 m for an average signal frequency of 1 kHz.

The receiver configuration consisted of an array of 12 dual-channel microstreamers, towed from a source-bearing modified catamaran (Fig. 1). The streamer spacing and the channel spacing within the streamers were both 1 m. Source and streamers were towed near the surface and offsets ranged between 6 m and 9 m. The catamaran was towed some 10 m behind the ship. During the survey a boomer and a modified watergun source were used. About 20 000 shots were recorded, each shot generating 24 seismic traces in a band 5.5 m wide along the tracks. Recording was done with an EGG seismograph, using a sampling rate of 0.25 ms. The shooting rate was 1 second.

In order to allow advanced processing, very accurate positioning was needed. This was done with an auto-tracking laser ranging theodolite, set up on the river bank, which continuously tracked a crown of reflector prisms mounted on top of the catamaran. This location reference point proved very stable due to the absence of

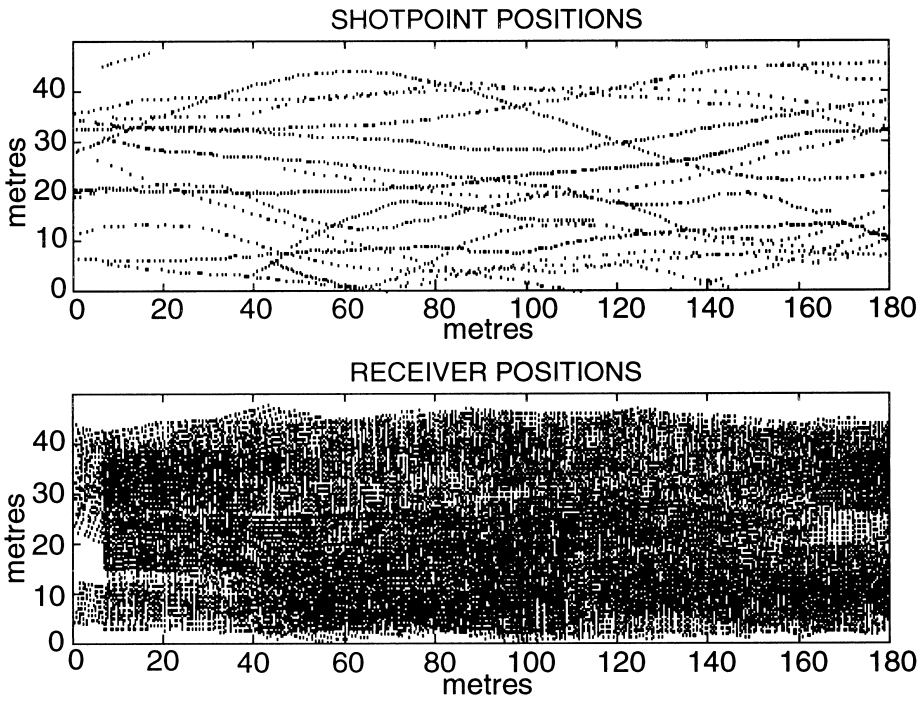

Figure 2. Geometry of source and receiver positions over the area of interest.

wave action (river environment). The measurement of transmission delay was taken into account when calculating the array positions. This full procedure resulted in a horizontal and vertical positioning accuracy of a few decimetres.

The strong tidal currents on the river, however, caused serious problems for the array stability. In order to keep the towed equipment well stretched behind the vessel, the seismic tracks were sailed against the current, alternately forwards and backwards, the latter simply by decreasing the speed. This procedure minimized relative positioning errors of the array. The absolute displacements over the ground varied considerably, resulting in a shot interval between 0.5 m and 2 m. Due to the currents and the sometimes busy river traffic, it was difficult to steer along the preplanned regularly spaced sail-lines. The latter were therefore adjusted in order to obtain a coverage as complete as possible.

Preliminary processing

The study presented here focused on a 50 m × 180 m area covering the diapir. Only the boomer data set (2000 shots, total data volume 70 Mb) will be discussed. The source and receiver locations were calculated from the prism positions taking into account the ship's movement, including the skew due to the currents. Due to the navigation problems mentioned above, the coverage with the boomer data was rather

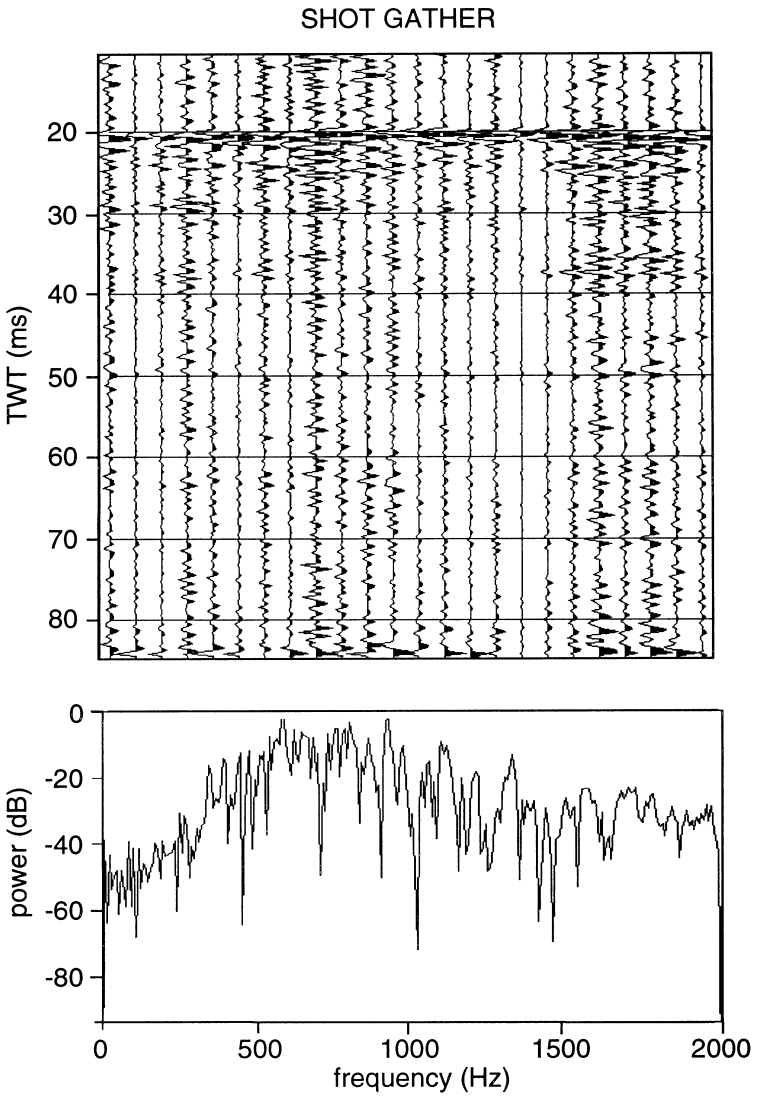

Figure 3. Top: example of one shot record after applying a band-pass filter and top mute. Below: corresponding amplitude spectrum.

variable. Although the coverage over the area of interest was fairly good in most parts, some areas (especially along the margin) were marked by relatively poor coverage (Fig. 2).

Data editing

The boomer source has a frequency range from a few hundred Hz up to well over

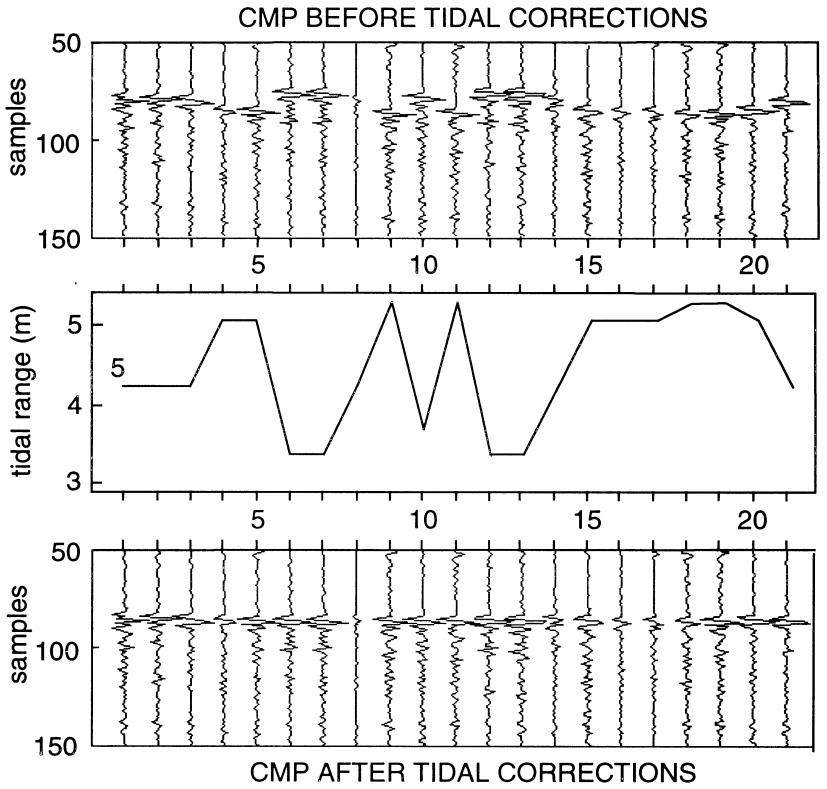

Figure 4. Top: example of one CMP (after NMO correction) before tidal correction. Middle: corresponding tidal amplitude. Below: same CMP after tidal correction.

2000 Hz. In view of the sampling rate, an antialias filter of 1400 Hz was applied during the survey. This limitation of the sampled frequency band has undoubtedly restricted the possible imaging resolution. It probably explains the absence on the 3D data of the above-mentioned clay concretions, the latter being automatically filtered out during digital recording. Since analogue recording can involve a much broader frequency range, it allowed observation of the diffraction hyperbolae on the paper records.

Band-pass filtering was carried out using a zero-phase Butterworth filter with half-power frequency of 400 Hz, and 40 dB/decade roll off at the slope. As the first part of each trace contained direct wave arrivals, a mute was applied before the river-bed reflection. Figure 3 shows a shot record of 24 traces after band-pass filtering (no NMO correction), and its corresponding average power spectrum. Due to the small offsets involved, the variation in arrival times between the different receivers is barely visible.

The sometimes strong variations in amplitude are due both to the lack of repetitivity of the source (inherent in broad-band, very high-frequency, seismic

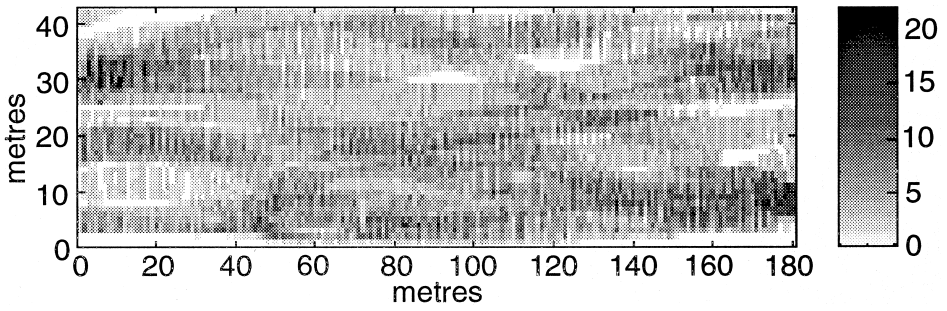

Figure 5. Stack fold coverage over the area of interest.

sources) and to the shallow immersion of source and receivers which cannot easily be monitored. Indeed, variations of a few decimetres in the towing depth will cause the original signal to interfere with its sea-surface ghost leading to frequency-dependent destructive summation. Therefore, no amplitude corrections were carried out on the data set.

Tidal correction

Tidal action on the river Schelde was quite large, with amplitudes up to 5.5 m (Fig. 4), whereas the dominant signal wavelength was less than 1 metre. Therefore the arrival times were corrected to a common level by adding a timeshift based on the vertical coordinate of the positioning prism crown (Fig. 4). These corrections were carried out on the zero-offset data, after the application of NMO assuming a constant velocity of 1500 m/s.

Multiple removal

The upper part of the clay diapir was marked by a relatively strong river-bed multiple. Due to the different tidal corrections, this multiple will be largely suppressed in the process of stacking. Nevertheless multiple removal was carried out through predictive deconvolution, using a Wiener–Levinson algorithm, applied on a trace-by-trace basis. The method applied proved to be quite efficient, resulting in a good suppression of the river-bed multiple.

Stacking

Taking into account the irregular navigation, NMO and stack had to be carried out using the exact locations of each source–receiver pair. Once the geometrical midpoint position had been computed for each trace, a stack grid was set out in bins of $1\,m \times 1\,m$ (Fig. 5). The resulting stack fold coverage appears rather heterogeneous over the survey area. According to the theoretical acquisition geometry a four-fold coverage should be obtained. Due to the irregular grid, however, the coverage was

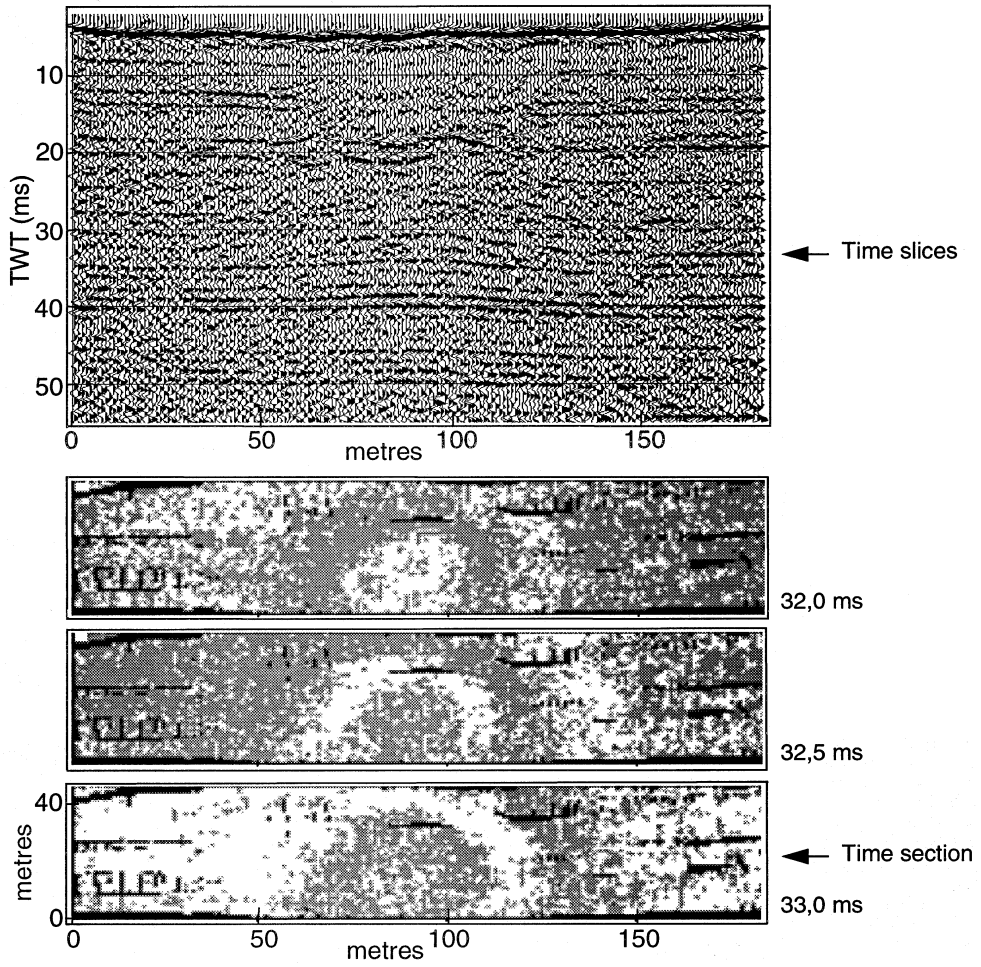

Figure 6. Results after stack. The time section is taken from a central row of bins. The time slices are separated by 0.5 ms.

high in some parts (up to 24 traces per bin), and consequently relatively poor in other parts.

The lack of large-offset data did not prevent the calculation of velocities using NMO-like analysis. Moreover, the small offsets and shallow depth of the target led to extremely small and almost constant Δt over the streamer array (from 4 to 6 samples). Therefore the NMO was carried out using velocity values extracted from geotechnical investigations (1500 m/s for the water column and 1600 m/s for the entire sediment column) (Heldens 1983). Such small variations in the P-wave velocity, as expected from the shallow depth, have very little effect on the imaging process. The actual stacking process was carried out per bin, resulting in a total of over 8000 stacks. The

full sequence of NMO and tidal corrections, geometry computations and stacking required 35 min on a Sparc 10 workstation.

The stacked data still displayed some high-frequency variations in the first-break arrivals. In order to correct for these time delays, and having no bathymetric control, the river-bed reflectors were smoothed by low-passing the first-break spatial wavelengths that were larger than the diameter of the Fresnel zone estimated for the average bathymetry, thus the traces were only shifted in time with a constant value. Although this resulted in a clear improvement in the upper few metres, the data quality decreased dramatically with depth. This suggests that the observed delays were most likely related to slight errors in the positioning of the acquisition array.

The results after stacking are shown in Fig. 6. The time section is chosen from a central row of bins, across the centre of the clay diapir. The time slices were taken from the lower part of the diapir (indicated by the arrow), and are separated by 0.5 ms. Due to the above-mentioned lack of information concerning the amplitudes, the time slices are simply represented in black and white, indicating the positive and negative phases.

The quality of the stacked section is good in the lower part of the diapir, with a large number of continuous and energetic reflectors visible. The middle and upper parts of the diapir, however, still remain quite disturbed, marked by discontinuous and incoherent reflectors. The time slices show the concentric reflector patterns growing towards the base of the diapir. Time slices above those shown in Fig. 6 were less and less coherent, which confirms the chaotic reflector pattern observed on the time section.

3D migration

Introduction

In order to obtain an accurate image of the clay diapir, and to improve the interpretability, the application of 3D migration is essential. The main benefit of migration concerns the removal of the propagation distortion from the reflectivity and the repositioning of the reflectors in their correct positions. The resulting improvement is most obvious for complex geological structures. For our specific data set acquired over a more-or-less 1D stratified medium, we do not expect dramatic geometrical changes nor quantitative information about the reflectivity.

A second benefit of migration concerns noise. The treatment of noise by migration algorithms has sometimes been neglected at the expense of the treatment of the signal, in spite of the fact that it can be of great importance. Migration reduces the amplitude of background noise without affecting the signal amplitudes. This is clearly demonstrated on our data set.

Migration processing is conventionally carried out after stacking. Post-stack migration is less costly as it involves a reduced volume of data, and is generally quite robust. In general, prestack migration gives more accurate results as it removes the cosine dependence of the stacking velocity on dip, forces spatial alignment and allows events of different dip at the same unmigrated time to stack correctly (Hatton,

Worthington and Makin 1986). However, this technique is less used in practice as it is often difficult to use and involves much higher processing costs due to the larger data volume. With increasingly powerful computers and new algorithms, the latter has become less of a disadvantage.

The question remains whether the results justify the costs. Algorithmically, full-waveform 3D depth migration before stack can be implemented, but it would incur an excessive computational cost. Fortunately, the objectives of shallow subsurface and geotechnical seismics are often not as exigent as those required by the oil industry. In terms of migration this means that we are mainly interested in the kinematics of how to reposition the reflectors of interest correctly. This allows a few approximations, which, in turn, allow a reduction in CPU time and the use of smaller computers, enabling us to circumvent the economic problem of migration.

Migration method

There are several approaches to migration. All have their own advantages and disadvantages, the proper choice depending upon the type of data to be migrated. For VHR small-scale 3D work, the main requirement is that it should be economical, and honour the kinematics. Furthermore, it should be able to handle the complex acquisition geometry (irregularly sampled spatial grid) easily. Considering these parameters, the Kirchhoff summation approach was the logical choice.

The Kirchhoff method can be interpreted as summing along diffraction curves. We look upon every point in the depth section as a possible diffractor. Since it is assumed that we know the velocity above this point, we can find the apex of its hypothetical diffraction hyperbola. Then we sum along this curve and place the value obtained at the given point.

When the medium does not have a constant velocity, the latter must be generalized. Essentially this amounts to replacing the straight ray traveltime by a traveltime accurately computed for a variable velocity medium. In this particular case, we used the algorithm introduced by Podvin and Lecomte (1991) which computes the first-arrival traveltimes by solving the eikonal equation by finite differences. This algorithm was used for both post-stack and prestack migration processing.

Migration processing requires a velocity model. The latter can normally be deduced from the stacking velocities obtained through conventional NMO processing. As mentioned above, this was not possible here due to the very short offsets which did not allow the picking of reliable stacking velocities. Instead the same 1D stratified velocity model was used as mentioned above for the NMO correction, based on geotechnical measurements at the tunnel site (Heldens 1983). Although this certainly represents an oversimplification of reality, the extremely shallow environment seems to justify this approximation.

Prestack migration

In order to prepare the data for prestack migration, an inverse NMO algorithm was applied to the tidal-corrected zero-offset data. The overall prestack migration

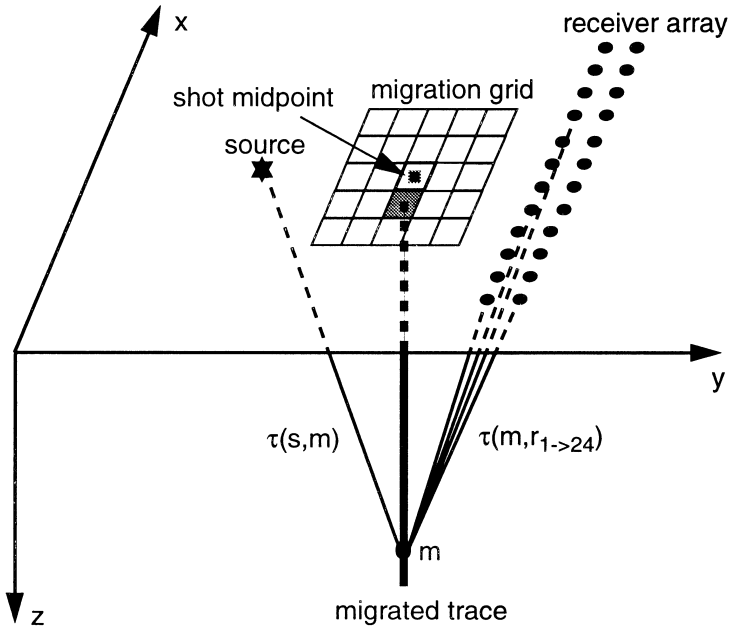

Figure 7. Geometry of the prestack migration (τ = traveltime).

operation involved the following steps: (1) computation of geometry parameters; (2) computation of the first time arrivals, and (3) summation migration.

In order to take into account our particular navigation pattern, we have tailored the Kirchhoff migration to meet our needs. Again, it should be emphasized how easily this particular migration handles both irregular shot and line spacing.

Prior to the migration itself, a grid with 1 m × 1 m bins is created. For a given aperture, the maximum offset (source-migrated trace or receiver-migrated trace) is calculated in order to compute the traveltime grid only once for the 1D velocity model we intend to use. This 2D time grid uses 0.1 m grid cells; the size of the cells was chosen with respect to the average wavelength of the seismic signal (less than one tenth).

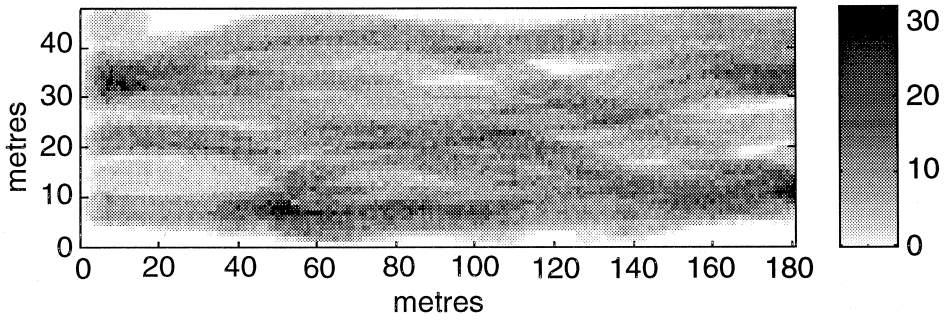

Figure 8. Post-migration stack fold coverage over the area of interest.

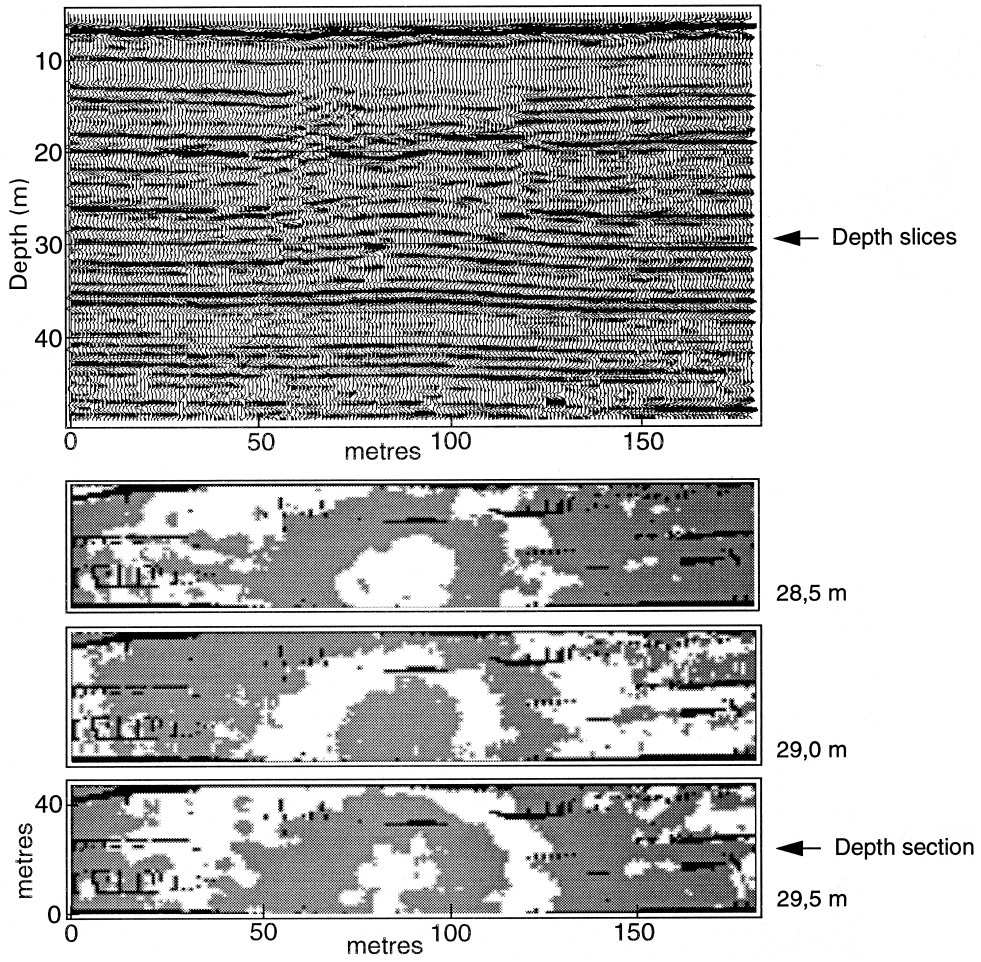

Figure 9. Results after post-stack migration. The depth section is taken from a central row of bins. The depth slices are separated by 0.5 m.

The migration is then carried out on a shot-by-shot basis. For each trace, migrated traces are calculated for the bins falling within the area centred around the corresponding CMP and extending up to the given aperture. In the case of an aperture of 10°, this roughly corresponds to 25 bins. Each migrated depth sample is evaluated as the sum of the 24 different trace values picked at the traveltimes corresponding to the (source–migrated trace–receiver) triplet (Fig. 7).

Migrated traces issued from different shots and located within the same bin are then summed together to form the final migrated volume. The resulting fold coverage was again rather heterogeneous over the survey area, with a maximum of 34 traces per bin (Fig. 8).

Preliminary tests were carried out using different apertures. The use of a large

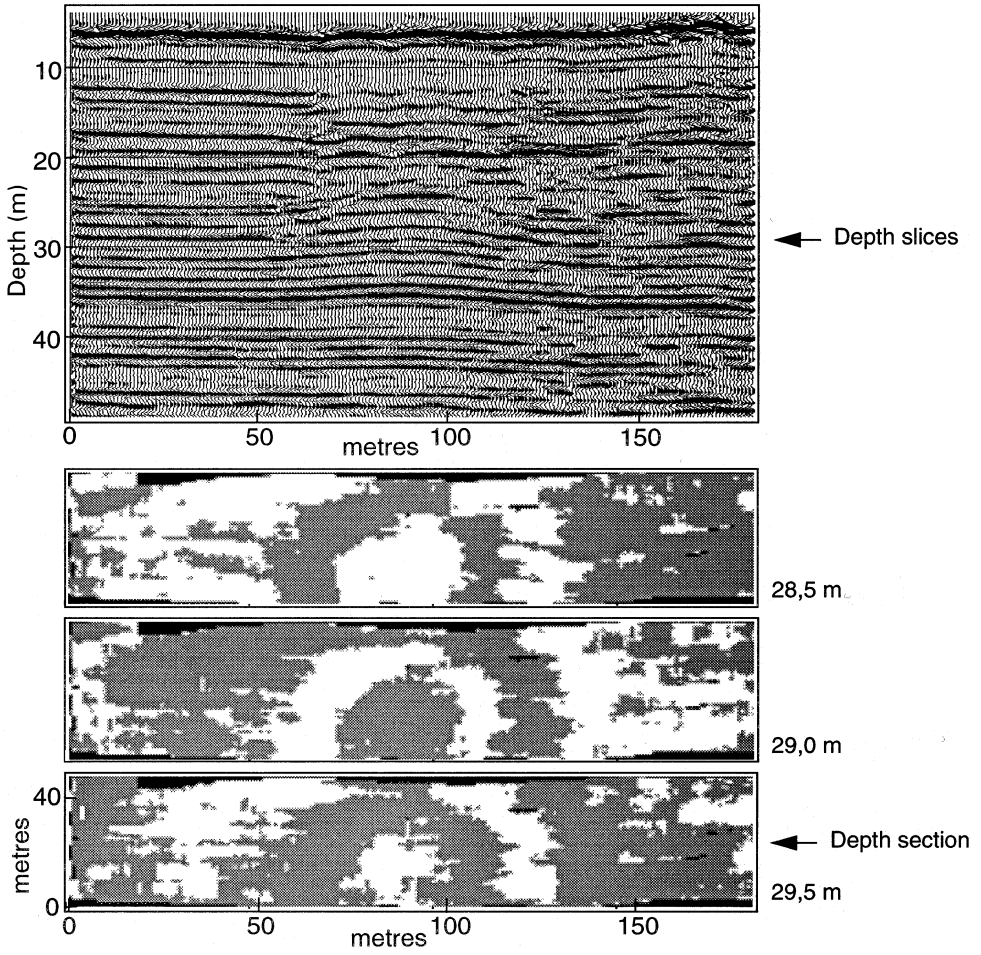

Figure 10. Results after prestack migration. The depth section is taken from a central row of bins. The depth slices are separated by 0.5 m.

aperture (more than 20°) dramatically increases the computing time while not adding new information to the results. Therefore a small aperture (10°) was used to produce the results discussed here. For the given aperture, the total processing time for inverse NMO and prestack migration on a Sparc 10 workstation was about 60 min, which includes the geometry calculations.

Post-stack migration

In order to compare the different migration methods, we also applied a 3D migration routine to the stacked data volume. The time grid used for the

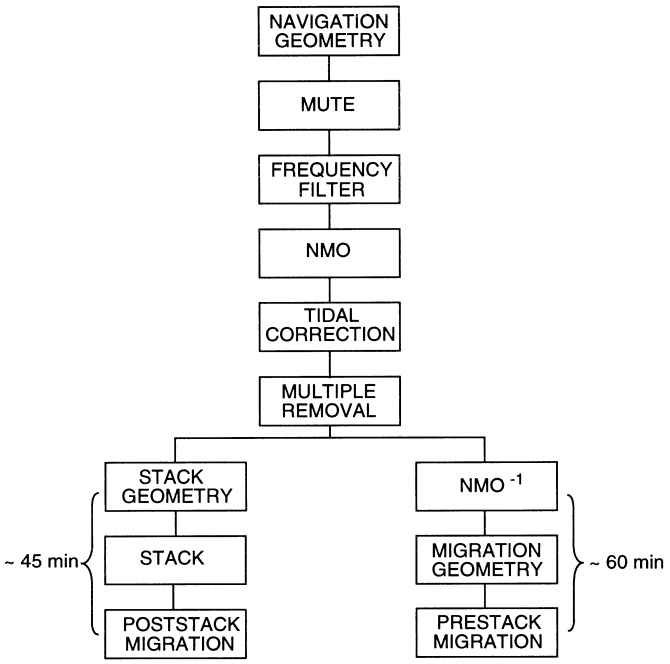

Figure 11. Different processing steps applied to the VHR 3D shallow marine data set.

calculation of the first-arrival traveltimes was the same as mentioned above. We therefore used an aperture equal to the coverage used for prestack migration.

The full sequence of stacking and post-stack migration required about 45 min on a Sparc 10 workstation, including NMO correction and the necessary stack geometry calculations.

Discussion

Figures 9 and 10 show the results after post-stack and prestack migration, in both cases for an aperture of 10°. The input data have been band-pass filtered and deconvolved to remove the multiple. The depth sections were chosen from a central row of bins, across the centre of the diapir. The depth slices, separated by 0.5 m, were taken from the lower part of the diapir (see arrow).

From these figures it is evident that both migration operations clearly improved the seismic image, even when based on a simple 1D stratified velocity model. In the latter case, however, the data improvement is mainly due to noise reduction and, to a lesser extent, the repositioning of the reflectors. The depth sections are marked by a large number of clearly distinguishable and coherent reflectors, which were still weak and distorted in the stack. The depth slices agree with these observations, as they are clearly marked by an improved resolution, with the concentric reflector pattern being better defined.

When comparing the post-stack and prestack results, we can see that the latter has better results. Indeed the continuity of the observed reflectors is better on the prestack migrated section, especially towards the middle part of the diapir. This is also the case for the corresponding depth slices, where the concentric reflector pattern is areally more restricted.

The uppermost part of the diapir, however, still remains somewhat chaotic. This seems to suggest that this part may have been subject to several gravitational collapses. Indeed the diapir growth may have induced stresses in the less undercompacted upper part of the clayey formation, causing overlying horizons to collapse into the initially undercompacted zone and destroying its internal strucure (Verschuren 1992).

Figure 11 gives an overview of the different processing steps applied to the VHR 3D shallow marine data set. The processing times involved were far from being excessive, even when carried out on a modest Sparc 10 workstation. In fact the extra CPU time for prestack migration was almost negligible compared to the post-stack sequence, whereas the latter produced less good results.

Conclusions

Very high resolution 3D seismics is of the greatest interest for detailed small-scale geological and geotechnical site investigations. The acquisition of VHR shallow 3D data has been demonstrated to be feasible, in a modest and cost-effective way, without requiring complex field procedures, and with bin sizes of the order of 1 metre. The processing of this small-scale 3D data volume implied challenging aspects related to the algorithmic treatment of the data, taking into account both the geotechnical goals and the processing facilities.

Prestack depth migration processing formed an important step in the processing sequence of the VHR 3D data volume. The algorithm used here was based on the Kirchhoff summation approach, using a 2D traveltime grid based on a 1D velocity model. The latter was possible due to the more-or-less stratified medium and the restricted data volume involved. With these approximations the prestack migration method applied proved very efficient, involving limited CPU time on a small workstation (Sparc 10), and clearly improving the interpretability of the data. This demonstrates that advanced seismic processing forms a valuable and economically feasible step in VHR 3D near-subsurface seismics, and there should no longer be any reason not to apply it.

Acknowledgements

The present study was partly carried out in the framework of an EEC MAST-II Research Fellowship (Project CT/5024/94). The development of the 3D acquisition system was supported by the EEC Directorate for Energy (Project TH/06036/87). The cooperation of the officers and crew of the RV Belgica is gratefully acknowledged.

References

Hatton L., Worthington M.H. and Makin J. 1986. *Seismic Data Processing*. Blackwell Scientific Publications.

Heldens P. 1983. *Een seismische studie van de klei van Boom en de klei van Ieper*. PhD thesis, University of Gent, Belgium.

Hemerijckx E., Carpentier R., De Schrijver P., Henriet J.P. and Heldens P. 1983. Preliminary investigations of concretion horizons in a Tertiary clay layer in view of the construction of a pre-metro tunnel under the river Scheldt at Antwerp (Belgium). Symposium on Engineering Geology and Underground construction, Lisbon, Proceedings I, 53–73.

Henriet J.P., Verschuren M. and Versteeg W. 1992. Very high resolution 3D seismic reflection imaging of small-scale structural deformation. *First Break* **10,** 81–88.

Podvin P. and Lecomte I. 1991. Finite difference computation of traveltimes in very contrasted velocity models: a massively parallel approach and its associated tools. *Geophysics* **105,** 271–284.

Schittekat J., Henriet J.P. and Vandenberghe N. 1983. Geology and geotechnique of the Scheldt surge barrier – characteristics of an oversolidated clay. Proceedings of the 8th International Harbour Congress, Antwerp (B), I.121–I.134.

Verschuren M. 1992. *An integrated 3D approach to clay tectonic deformation*. PhD thesis, University of Gent, Belgium.